Displacement-based formation control with disturbance observer of multi-first-order systems

Dao Thi My Linh[1,3], Nguyen Hoai Nam [1,*], Pham Van Thiem [2]

[1]Hanoi University of Science and Technology
[2]Phenikaa University
[3]Thai Binh University
[*]nam.nguyenhoai@hust.edu.vn
DOI: https://doi.org/10.64032/mca. v30i4.432

Abstract

This paper addresses the problem of displacement-based formation control for multi-agent systems with first-order integrator dynamics in the presence of external disturbances. Based on the proposed control law, a disturbance observer is developed to estimate the disturbances acting on each agent, and the estimated signals are incorporated into the control input for disturbance compensation. This approach enables the system to maintain the desired formation while enhancing its disturbance rejection capability. Lyapunov-based stability analysis shows that the formation error is uniformly ultimately bounded when the disturbance estimation error is bounded. Furthermore, if the estimation error converges to zero over time, the formation error asymptotically converges to zero. Simulation results on a five-agent system validate the effectiveness of the proposed method, demonstrating a significant reduction in formation error and improvement of system performance compared to the case without the disturbance observer.

***Keywords**: Displacement-based; Disturbance observer; Formation control; Multi-agent systems; Single-integrator systems*

Abbreviations

MAS	Multi-Agent-Systems
DOB	Disturbance-Observer-Based
UUB	Uniformly Ultimately Bounded

1. Introduction

Multi-agent systems have been widely studied in applications such as UAV formation control, cooperative robotics, and distributed autonomous systems because they can achieve coordinated behaviors through local interactions among agents [1], [2]. Formation control is a fundamental coordination problem that aims to maintain a desired geometric configuration during motion [3]–[6]. Existing approaches are commonly classified into position-based [7], [8], displacement-based [9]–[11], distance-based [12], [13], bearing-based [14], [15], and angle-based methods [16], [17]. Among these approaches, displacement-based formation control specifies the desired formation through prescribed relative-position vectors between neighboring agents over the interaction graph. Because each displacement vector contains both magnitude and directional information, this approach directly specifies the desired relative-position relationships among the agents, rather than representing the formation through separate distance, bearing, or angle constraints [5], [14], [16]. When the prescribed displacement constraints are feasible, an appropriate distributed controller can drive the agents to the desired configuration up to a common translation [5]. Recent work has also extended this framework to range-only sensing using data-driven estimation of relative-position and orientation information [18]. Within the first-order setting considered in this study, the displacement-based representation naturally yields consensus-type formation-error dynamics, thereby facilitating distributed controller design and convergence analysis [19].

Nevertheless, in practical applications, multi-agent systems are inevitably affected by external disturbances, which may increase formation errors and degrade closed-loop performance. To mitigate these effects, various robust-control and disturbance-rejection techniques have been developed [20]–[22]. Among them, disturbance-observer-based control provides a systematic framework for estimating unknown disturbances online and compensating for their effects through the control input [20], [21]. Disturbance-rejection mechanisms have also been investigated for different formation-control architectures, including distributed active disturbance rejection for quadrotor formation tracking [22], robust control for bearing-constrained formations [24], angle-constrained formation control with disturbance rejection [17], and distributed disturbance compensation for displacement-based formations of first-order integrator agents [26]. These studies differ in their geometric constraints, agent dynamics, disturbance assumptions, and compensation mechanisms. Among them, [26] is most closely related to the present study because it considers displacement-based formations of first-order integrator agents subject to unknown disturbances and develops a distributed compensation mechanism with prescribed disturbance-rejection performance.

Received: 21 April 2026; Revised: 5 August 2026; Accepted: 10 August 2026.

In this study, the first-order integrator model is adopted as a basic framework to focus on the disturbance-estimation and compensation mechanism. Specifically, a disturbance observer is incorporated into a displacement-based formation controller to estimate and compensate for the disturbance acting on each agent.

The main contribution of this work is a Lyapunov-based stability analysis of the proposed observer-based formation control scheme under unknown time-varying disturbances with bounded derivatives. Explicit ultimate bounds are derived for both the disturbance-estimation error and the formation error. For constant disturbances, the disturbance-estimation error converges exponentially to zero, leading to the asymptotic convergence of the formation error. Comparative simulations with a controller without disturbance compensation and the reference method in [26] are conducted to evaluate the effectiveness of the disturbance-rejection and control performance of the proposed method.

The remainder of this paper is organized as follows. Section 2 presents the theoretical preliminaries. Section 3 develops the formation controller and disturbance observer. Section 4 provides stability analysis. Section 5 presents the simulation results and discussion. Finally, Section 6 concludes the paper.

2. Theoretical preliminaries

2.1 Graph theory

Consider an undirected weighted graph $\mathcal{G} = (\mathcal{V}, E)$, where $\mathcal{V} = \{1,2 \dots, n\}$ denotes the set of agents and $E \subseteq \mathcal{V} \times \mathcal{V}$ denotes the set of edges describing the information exchange links among agents. If $(i,j) \in E$, agents i and j can exchange relative information. The neighbor set of agent i is defined as $\mathcal{N}_i = \{j \in \mathcal{V}: (i,j) \in E\}$

The interaction topology of the system is characterized by the Laplacian matrix [23] $L = [\ell_{ij}] \in \mathbb{R}^{n \times n}$, whose entries are defined as

$$\ell_{ij} = \begin{cases} -a_{ij}, i \neq j \\ \sum_{j=1}^{n} a_{ij}, i = j \end{cases}$$

where $a_{ij} > 0$ denotes the weight associated with the edge agents i and j. For an undirected weighted graph, the adjacency weights satisfy $a_{ij} = a_{ji}, a_{ii} = 0, a_{ij} > 0$ if and only if $(i,j) \in E$; otherwise, $a_{ij} = 0$

Consequently, the Laplacian matrix L is symmetric and positive semidefinite.

Assumption 1. The interaction graph $\mathcal{G}$ is fixed, undirected, and connected.

Under Assumption 1, the Laplacian matrix L has a simple zero eigenvalue, and its eigenvalues satisfy

$$0 = \lambda_1(L) < \lambda_2(L) \leq \cdots \leq \lambda_n(L),$$

where, $\lambda_2 > 0$ is the second-smallest eigenvalue of L, also referred to as the algebraic connectivity of the interaction graph.

Moreover, since $\mathcal{G}$ is connected, 0 is a simple eigenvalue of L and $L\mathbf{1}_n = 0$, where $\mathbf{1}_n = [1, \dots, 1]^\top \in \mathbb{R}^n$

For notational convenience, I_q denotes the $q \times q$ identity matrix, $\otimes$ is the Kronecker product, and $\|\cdot\|$ is the Euclidean norm.

2.2 Agent kinematic model

Consider a multi-agent system consisting of n agents moving in a q-dimensional Euclidean space. The position dynamics of each agent are described by the following q-dimensional first-order integrator subject to external disturbances [24]:

$$\dot{p}_i = u_i + d_i, \ i = 1, \dots, n. \tag{1a}$$

Here, $p_i \in \mathbb{R}^q, u_i \in \mathbb{R}^q, d_i \in \mathbb{R}^q$ denote the position vector, control-input vector, and external-disturbance vector of agent i, respectively, where q is the dimension of the physical space. The stacked position, control-input, and disturbance vectors of the overall multi-agent system are defined as $p = [p_1^\top \ p_2^\top \dots p_n^\top]^\top \in \mathbb{R}^{nq}$, $u = [u_1^\top \ u_2^\top \dots u_n^\top]^\top \in \mathbb{R}^{nq}$, and $d = [d_1^\top \ d_2^\top \dots d_n^\top]^\top \in \mathbb{R}^{nq}$, respectively. Accordingly, the stacked dynamics of the multi-agent system are expressed as

$$\dot{p} = u + d \tag{1b}$$

Assumption 2. For each agent i, the disturbance $d_i(t)$ is continuously differentiable. Moreover, there exist finite nonnegative constants $\bar{d}_i \geq 0$ and $\bar{\rho}_i \geq 0$ such that

$$\|d_i(t)\| \leq \bar{d}_i, \ \|\dot{d}_i(t)\| \leq \bar{\rho}_i, \forall t \geq 0. \tag{2}$$

where $\bar{d}_i$ and $\bar{\rho}_i$ denote upper bounds on the disturbance and its time derivative, respectively.

2.3 Displacement-based formation control

The nominal displacement-based formation controller uses relative displacement information between neighboring agents. For each edge $(i,j) \in E$, the relative displacement from agent i to j is defined as

$$z_{ij} = p_j - p_i. \tag{3a}$$

Let

$$\Gamma = \{z_{ij}^*\}_{(i,j) \in E} \tag{3b}$$

be a set of prescribed relative displacement vectors defining the desired formation.

Assumption 3. The desired relative displacement constraints are time-invariant and mutually consistent. Specifically, there exists at least one stationary configuration

$$p^* = [p_1^{*T} \ p_2^{*T} \ \cdots \ p_n^{*T}]^T \in \mathbb{R}^{nq}$$

such that

$$p_j^* - p_i^* = z_{ij}^*, \forall (i,j) \in E. \tag{4}$$

The control objective is to ensure

$$z_{ij}(t) - z_{ij}^* \to 0, \quad \forall (i,j) \in E.$$

Define the position-error vector of the agent i as

$$\delta_i = p_i^* - p_i \in \mathbb{R}^q \tag{5}$$

and the corresponding stacked vector as

$$\delta = [\delta_1^\top \ \delta_2^\top \dots \delta]^\top = p^* - p \in \mathbb{R}^{nq},$$

Under Assumptions 1 and 3, the nominal displacement-based formation-control law for the agent i is given by

$$u_i = k_p \sum_{j \in N_i} a_{ij} \left[(p_j - p_i) - (p_j^* - p_i^*) \right], \tag{6a}$$

where $k_p > 0$ is the control gain.

In stacked form, the nominal control law is expressed as

$$u = k_p (L \otimes I_q) \delta \tag{6b}$$

In the disturbance-free case, the corresponding position-deviation dynamics are

$$\dot{\delta} = -\dot{p} = -k_p(L \otimes I_q)\delta, \tag{7a}$$

Define the Laplacian-based formation-error vector as

$$\varepsilon = (L \otimes I_q)\delta \in \mathbb{R}^{nq}. \tag{7b}$$

Therefore, $\varepsilon = 0$ implies that all prescribed relative displacement constraints are satisfied. Because L has a simple zero eigenvalue, $\varepsilon = 0$ does not necessarily imply $\delta = 0$. Instead, the desired formation is established up to a common translation.

3. Disturbance observer design

Assumption 4. Each agent i can measure the relative displacements $p_j - p_i, j \in \mathcal{N}_i$ and can obtain its own position p_i in a common reference frame. The absolute positions and disturbance estimates of neighboring agents are not required.

Although the displacement-based formation controller relies on relative displacement measurements, the proposed disturbance observer requires the absolute position p_i of each agent expressed in a common reference frame. Therefore, its implementation depends on an onboard or external localization system, which may limit its applicability in environments where reliable absolute localization is unavailable.

To estimate the unknown disturbance d_i without directly differentiating the measured position p_i, an auxiliary state $\eta_i \in \mathbb{R}^q$, is introduced. Following the disturbance-observer structure proposed by Chen [21], the disturbance estimate is designed as

$$\hat{d}_i = \eta_i + \gamma p_i, \tag{8}$$

where the auxiliary-state dynamics are given by

$$\dot{\eta}_\iota = -\gamma\eta_i - \gamma(\gamma p_i + u_i). \tag{9}$$

Here, $\hat{d}_i \in \mathbb{R}^q$ denotes the disturbance estimation of agent i, and $\hat{d} = [\hat{d}_1^\top, \dots, \hat{d}_n^\top]^\top \in \mathbb{R}^{nq}$ denotes the stacked disturbance-estimate vector of all agents, and $\gamma > 0$ is the observer gain.

Taking the time derivative of (8), one gets

$$\dot{\hat{d}}_\iota = \dot{\eta}_\iota + \gamma\dot{p}_\iota, \tag{10}$$

Substituting (2) and (9) into (10) and simplifying yields

$$\begin{aligned}\dot{\hat{d}}_i &= -\gamma\eta_i - \gamma(\gamma p_i + u_i) + \gamma(u_i + d_i)\\ &= -\gamma(\eta_i + \gamma p_i) + \gamma d_i\\ &= -\gamma\hat{d}_i + \gamma d_i\\ &= \gamma(d_i - \hat{d}_i).\end{aligned} \tag{11}$$

The disturbance-estimation error of the agent i is defined as

$$\tilde{d}_i = d_i - \hat{d}_i \in \mathbb{R}^q \tag{12}$$

For the overall multi-agent system, the stacked disturbance-estimation error vector is defined as

$$\tilde{d} = [\tilde{d}_1^\top, \dots, \tilde{d}_n^\top]^\top \in \mathbb{R}^{nq}$$

Using (11), the disturbance-estimation-error dynamics of the agent i are given by

$$\dot{\tilde{d}}_\iota = -\gamma\tilde{d}_i + \dot{d}_\iota. \tag{13}$$

Therefore, the disturbance-estimation-error dynamics of the overall multi-agent system are given by

$$\dot{\tilde{d}} = -\gamma\tilde{d} + \dot{d}, \tag{14}$$

where

$$\dot{d} = [\dot{d}_1^\top\ \dot{d}_2^\top \dots \dot{d}_n^\top]^\top \in \mathbb{R}^{nq}$$

Based on the estimated disturbance, the proposed disturbance-compensated formation-control law is given by

$$u = k_p(L \otimes I_q)\delta - \hat{d} \tag{15}$$

The first term in (15) is the nominal displacement-based formation control term, whereas the second term compensates for the disturbances.

Substituting (15) into the stacked agent dynamics (1b) yields

$$\begin{aligned}\dot{p} &= k_p(L \otimes I_q)\delta - \hat{d} + d\\ \dot{p} &= k_p(L \otimes I_q)\delta + \tilde{d}.\end{aligned} \tag{16}$$

For the stationary desired formation and the position-error definition $\delta = p^* - p$, one has $\dot{p}^* = 0$. Therefore, the closed-loop position-error dynamics are

$$\dot{\delta} = -k_p(L \otimes I_q)\delta - \tilde{d}. \tag{17}$$

4. Stability analysis

4.1 Disturbance observer

From he stacked disturbance-estimation-error dynamics in (14), consider the Lyapunov candidate function:

$$V_1 = \tfrac{1}{2}\tilde{d}^T\tilde{d}. \tag{18}$$

The function V_1 is positive definite with respect to $\tilde{d}$.

Its time derivative along the trajectories of the estimation-error system is

$$\dot{V}_1 = \tilde{d}^T\dot{\tilde{d}} \tag{19}$$

Using the stacked estimation-error dynamics gives

$$\dot{V}_1 = -\gamma\|\tilde{d}\|^2 + \tilde{d}^T\dot{d}. \tag{20}$$

By Young's inequality

$$\tilde{d}^T\dot{d} \le \tfrac{\gamma}{2}\|\tilde{d}\|^2 + \tfrac{1}{2\gamma}\|\dot{d}\|^2. \tag{21}$$

Consenquently,

$$\dot{V}_1 \le -\tfrac{\gamma}{2}\|\tilde{d}\|^2 + \tfrac{1}{2\gamma}\|\dot{d}\|^2. \tag{22}$$

From Assumption 2 and the definition of $\dot{d}(t)$ in (14), we obtain

$$\begin{aligned}\|\dot{d}(t)\| &= \sqrt{\sum_{i=1}^{n}\|\dot{d}_i(t)\|^2}\\ &\le \sqrt{\textstyle\sum_{i=1}^{n}\bar{\rho}_i^2} \triangleq \bar{\rho}, \quad \forall t \ge 0.\end{aligned} \tag{23}$$

Substituting (23) into (22) yields

$$\dot{V}_1 \le -\tfrac{\gamma}{2}\|\tilde{d}\|^2 + \tfrac{\bar{\rho}^2}{2\gamma} \tag{24}$$

It follows from (24) that

$$\dot{V}_1 < 0 \text{ whenever } \|\tilde{d}\| > \tfrac{\bar{\rho}}{\gamma}. \tag{25}$$

Therefore, the disturbance-estimation error is uniformly ultimately bounded and satisfies

$$\limsup_{t\to\infty}\|\tilde{d}(t)\| \le \tfrac{\bar{\rho}}{\gamma} \tag{26}$$

If the disturbances are constant, then $\dot{d} = 0$, and (22) reduces to

$$\dot{V}_1 \le -\gamma V_1,$$

which implies that $\tilde{d}$ converges exponentially to zero. For time-varying disturbances with bounded derivatives, the bound of the estimation-error decreases as γ increases. However, an excessively large observer gain may increase sensitivity to position-measurement noise.

4.2 Formation error

Differentiating (7b) yields

$$\dot{\varepsilon} = (L \otimes I_q)\dot{\delta}. \tag{27}$$

Substituting the closed-loop position-error dynamics (17) into (27) yields

$$\begin{aligned}\dot{\varepsilon} &= (L \otimes I_q)\left[-k_p(L \otimes I_q)\delta - \tilde{d}\right] \\ &= -k_p(L \otimes I_q)(L \otimes I_q)\delta - (L \otimes I_q)\tilde{d}\end{aligned}$$

Using (7b), one obtains

$$\dot{\varepsilon} = -k_p(L \otimes I_q)\varepsilon - (L \otimes I_q)\tilde{d}. \tag{28}$$

The matrix product in the second line is equivalent to L^2, since

$$(L \otimes I_q)(L \otimes I_q) = L^2 \otimes I_q$$

Consider the Lyapunov function:

$$V_2(t) = \frac{1}{2}\varepsilon^T\varepsilon = \frac{1}{2}\|\varepsilon\|^2. \tag{29}$$

The function V_2 is positive definite with respect to ε. Its time derivative is

$$\dot{V}_2 = \varepsilon^T\dot{\varepsilon}. \tag{30}$$

Using (28), one obtains

$$\dot{V}_2 = -k_p\varepsilon^T(L \otimes I_q)\varepsilon - \varepsilon^T(L \otimes I_q)\tilde{d}. \tag{31}$$

Because $\mathcal{G}$ is undirected and connected, the Laplacian matrix L is symmetric and positive semidefinite. Moreover, since $\varepsilon \in \text{range}(L \otimes I_q)$, and $L \otimes I_q$ is symmetric, ε is orthogonal to its null space. Therefore,

$$\varepsilon^T(L \otimes I_q)\varepsilon \geq \lambda_2\|\varepsilon\|^2. \tag{32}$$

Furthermore, by the Cauchy–Schwarz inequality and the spectral properties of the symmetric Laplacian matrix,

$$\begin{aligned}\left|\varepsilon^T(L \otimes I_q)\tilde{d}\right| &\leq \|\varepsilon\|\left\|(L \otimes I_q)\tilde{d}\right\| \\ &\leq \lambda_n\|\varepsilon\|\left\|\tilde{d}\right\|,\end{aligned} \tag{33}$$

where λ_n denotes the largest eigenvalue of L.

Substituting (32) and (33) into (31) yields

$$\dot{V}_2 \leq -k_p\lambda_2\|\varepsilon\|^2 + \lambda_n\|\varepsilon\|\left\|\tilde{d}\right\|. \tag{34}$$

Equivalently,

$$\dot{V}_2 \leq -\|\varepsilon\|(k_p\lambda_2\|\varepsilon\| - \lambda_n\left\|\tilde{d}\right\|). \tag{35}$$

Hence, $\dot{V}_2 < 0$ whenever

$$\|\varepsilon\| > \frac{\lambda_n}{k_p\lambda_2}\left\|\tilde{d}\right\| \tag{36}$$

Since the disturbance-estimation error is uniformly ultimately bounded according to (26), it follows from (36) that the formation error ε is also uniformly ultimately bounded. In particular,

$$\begin{aligned}\limsup_{t\to\infty}\|\varepsilon(t)\| &\leq \frac{\lambda_n}{k_p\lambda_2}\limsup_{t\to\infty}\left\|\tilde{d}(t)\right\| \\ &\leq \frac{\lambda_n\bar{\rho}}{k_p\lambda_2\gamma}.\end{aligned}$$

Therefore, the ultimate bound on the formation-error decreases when either formation-control gain k_p or the observer gain γ, or both, are increases. Regarding the communication topology, the bound becomes smaller as the spectral ratio $\frac{\lambda_n}{\lambda_2}$ decreases. In contrast, faster disturbance variations, characterized by a larger value of $\bar{\rho}$, result in a larger ultimate formation-error bound.

For constant disturbances, $\dot{d} = 0$, and the disturbance-estimation error converges exponentially to zero. Since the homogeneous part of the formation-error dynamics in (28) is exponentially stable on $\text{range}(L \otimes I_q)$, it follows that

$$\tilde{d}(t) \to 0 \Rightarrow \varepsilon(t) \to 0$$

Thus, the formation error of the overall multi-agent system asymptotically converges to zero. However, owing to the translational invariance of displacement-based formation control, $\varepsilon(t) \to 0$ does not necessarily imply $\delta(t) \to 0$. Instead, it implies that the position-error vector asymptotically approaches the null space of $L \otimes I_q$ corresponding to a common translational offset shared by all agents.

5. Simulation results and discussion

To evaluate the effectiveness of the proposed method, numerical simulations are carried out on a first-order multi-agent system composed of $n = 5$ agents evolving in a three-dimensional space, *i.e.*, $p_i \in \mathbb{R}^3$, $i = 1, \ldots, n$. The interaction topology is selected as a cyclic graph. The associated oriented incidence matrix is defined as

$$H = \begin{vmatrix} -1 & 1 & 0 & 0 & 0 \\ 0 & -1 & 1 & 0 & 0 \\ 0 & 0 & -1 & 1 & 0 \\ 0 & 0 & 0 & -1 & 1 \\ 1 & 0 & 0 & 0 & -1 \end{vmatrix} \tag{37}$$

and the corresponding Laplacian matrix is given by

$$L = H^T H. \tag{38}$$

The corresponding three-dimensional form is given by:

$$L_q = L \otimes I_3.$$

The desired formation is chosen as a five-point star lying on the plane $z = \frac{\pi}{2}$ with radius 5. Specifically, the desired position of the *i-th* agent is given by:

$$p_i^* = \begin{vmatrix} 5cos\theta_i \\ 5\,sin\theta_i \\ \frac{\pi}{2} \end{vmatrix}, \theta_i \in \{0°, 144°, 288°, 72°, 216°\}.$$

The initial agent positions are randomly generated in the interval $[-10,10]$ for each coordinate component, while the initial state of the disturbance observer is set to zero. To ensure reproducibility, the random seed is fixed as $rng(1)$. The simulation interval is chosen as $0 \leq t \leq 80\,s$ with a sampling step of $0.001\,s$.

In this simulation, the external disturbance acting on each agent is assumed to be time-varying and agent-dependent. The disturbance amplitude is increased at $t = 40s$ to assess the response of the closed-loop system when the disturbance environment suddenly becomes more adverse. Specifically, for the agent i, the disturbance is defined as follows:

$$d_i(t) = a(t)\begin{vmatrix} \sin(it) + 1 \\ \cos(it) + \tanh(t) \\ 1 - e^{-it} \end{vmatrix}, \tag{39}$$

where a(t) denotes the disturbance amplitude:

$$a(t) = \begin{cases} 0.1, t < 40 \\ 0.15, t \geq 40 \end{cases}$$

To quantitatively evaluate the formation-control performance, control effort, and disturbance-estimation error, the RMS, MAE, IAE, and ITAE metrics of the formation error, together with the RMS values of the control input and disturbance-estimation error, are calculated according to (40).

$$RMS_\varepsilon = \sqrt{\frac{1}{N}\sum_{k=1}^{N}\|\varepsilon(t_k)\|^2},$$

$$MAE_\varepsilon = \frac{1}{N}\sum_{k=1}^{N}\|\varepsilon(t_k)\|,$$

$$IAE_\varepsilon = \Delta t\sum_{k=1}^{N}\|\varepsilon(t_k)\|,$$

$$ITAE_\varepsilon = \Delta t\sum_{k=1}^{N}\tau_k\|\varepsilon(t_k)\|, \tau_k = (k-1)\Delta t,$$

$$RMS_u = \sqrt{\frac{1}{N}\sum_{k=1}^{N}\|u(t_k)\|^2},$$

$$RMS_{\tilde{d}} = \sqrt{\frac{1}{N}\sum_{k=1}^{n}\left\|\tilde{d}(t_k)\right\|^2}. \quad (40)$$

Here, t_k denotes the k^{th} sampling instance, N is the number of samples in each evaluation interval, $\Delta t = 0.001s$is the uniform sampling interval, and τ_k is the local elapsed time corresponding to the k_{th}.

The simulation results are presented in Figs. 1-8. In addition, we use several performance metrics to quantitatively evaluate the effectiveness of the controller. These include the formation error norm $\|\varepsilon(t)\|$, the control input norm $\|u(t)\|$, the disturbance estimation performance is evaluated through $\|d(t)\|$, $\|\hat{d}(t)\|$and $\|\tilde{d}(t)\|$for each agent and for the overall network. Finally, the agent trajectories and the variations of these quantities around $t = 40s$ are used to highlight the disturbance-rejection capability of the system.

In addition, the proposed controller is compared with two reference cases: the baseline controller without a disturbance observer and the controller reported in [26]. The comparison results are presented in Table 1.

Table 1: Comparison of control performance.

Time in-terval	Controller	RMS1_ε(t)	MAE_ε(t)	IAE_ε(t)	ITAE_ε(t)	RMS2_u(t)	RMS3_d̃(t)
0-40 s	No DOB	2.4178	0.29664	11.866	54.316	6.0446	NaN
0-40 s	**DOB**	**1.736**	**0.13509**	**5.4036**	**6.9816**	**14.744**	**12.731**
0-40 s	Reference method [26]	1.6064	0.094699	3.7881	15.431	12.041	NaN
40-80 s	No DOB	0.10456	0.10052	4.0207	80.629	0.2614	NaN
40-80 s	**DOB**	**0.012636**	**0.012205**	**0.48821**	**9.7824**	**0.67506**	**0.044137**
40-80 s	Reference method [26]	0.030203	0.029083	1.1633	23.311	0.30095	NaN
0-80 s	No DOB	1.7113	0.19858	15.887	295.78	4.2782	NaN
0-80 s	**DOB**	**1.2276**	**0.073647**	**5.8918**	**36.293**	**10.437**	**9.0022**
0-80 s	Reference method [26]	1.1361	0.061892	4.9514	85.277	8.5168	NaN

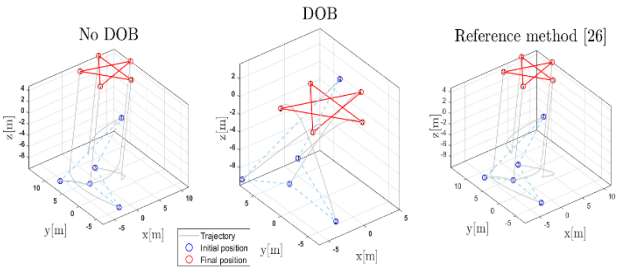


Figure 1: Agent trajectories and final formation shape

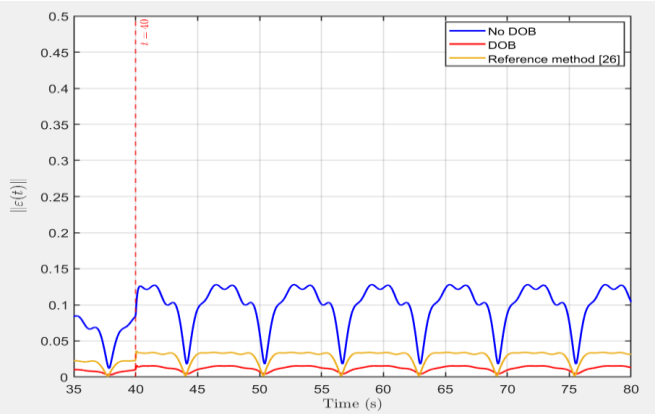


Figure 2: Formation error versus time.

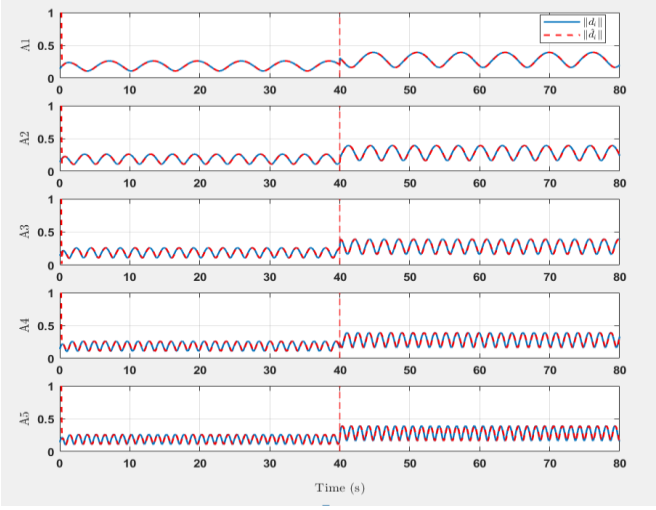


Figure 3: True and estimated disturbance norms for each agent

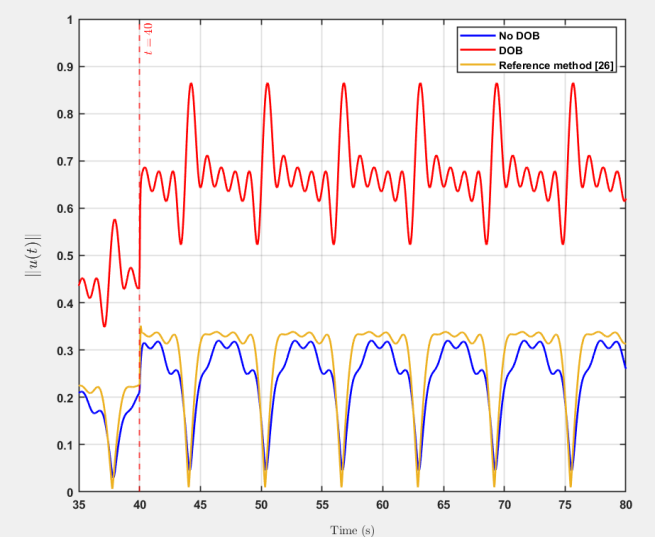


Figure 4: Time response of the control input norm

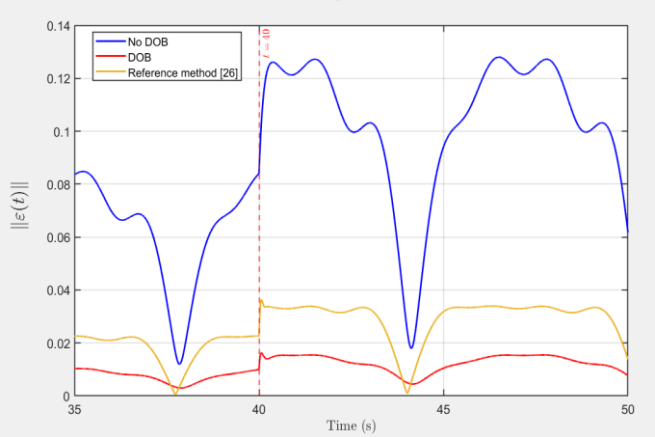


Figure 5: Zoomed view of the formation error around t = 40 s

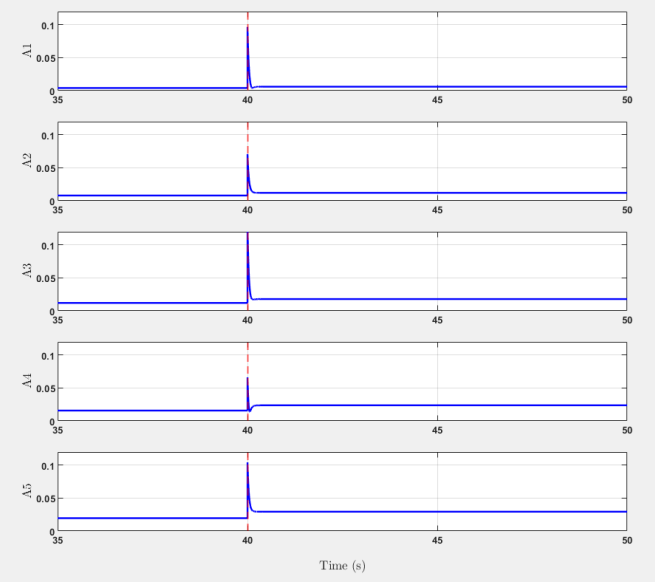


Figure 6: Zoomed view of the disturbance estimation error around t = 40 s

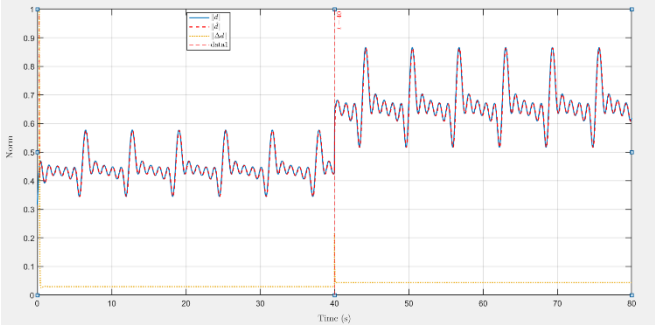


Figure 7: Disturbance estimation performance

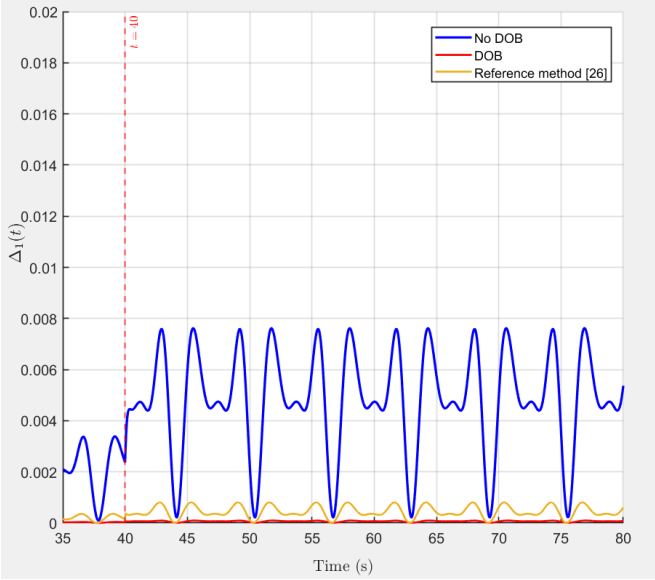


Figure 8: Time response of the edge-based formation error

Table 1 presents the quantitative formation-control performance of the three considered controllers. During the initial interval $0 - 40\ s$ the DOB-based controller reduces the RMS formation error by 28.2%, the MAE and IAE by approximately 54.5%, and the ITAE by 87.1% compared with the controller without disturbance estimation. Although the method [26] provides lower RMS, MAE, and IAE values during this transient interval, the proposed controller yields the smallest ITAE, indicating faster convergence of formation errors.

When the disturbance amplitude increases at $t = 40\ s$, the advantage of the DOB-based controller becomes more evident. Over $40 - 80\ s$, its RMS formation error is 0.0126, which is 87.9% lower than that of the controller without disturbance estimation and 58.2% lower than that of the method [26]. Similar reductions are also obtained for the MAE, IAE, and ITAE indices. The RMS disturbance-estimation error decreases from 12.731 during the initial interval to 0.044 after $t = 40\ s$, showing that the large estimation error is mainly associated with the initial observer transient. These improvements are achieved with a higher RMS for the control input, confirming the trade-off between disturbance rejection and control effort.

Over the entire interval $0 - 80\ s$, the reference method produces slightly lower RMS, MAE, and IAE values than the proposed controller because these indices are strongly affected by the initial transient. Nevertheless, the proposed

controller achieves the lowest ITAE value 36.293, compared with 85.277 for the reference method as well as for the controller without disturbance estimation. This result indicates that the DOB-based controller is particularly effective in suppressing formation errors that persist at later sampling instances.

6. Conclusion

In this paper, a disturbance-observer-based displacement formation control scheme was proposed for first-order multi-agent systems subject to external disturbances. The proposed approach integrates a disturbance observer into the formation control law to estimate and compensate for the disturbances acting on each agent. Stability analysis proves that both the disturbance-estimation error and the formation error are uniformly ultimately bounded. Comparative simulations results demonstrate significant improvements of disturbance-rejection capacity and control performance. Although these improvements are achieved at the cost of higher control effort, the overall results confirm the effectiveness of the proposed approach in disturbed environments.

The proposed method still has several limitations regarding real-time implementation. The first-order model does not fully capture practical UAV dynamics, while the disturbance observer requires absolute position measurements, which may restrict its applicability in environments where reliable absolute localization is unavailable. In addition, actuator constraints, measurement noise, and communication failures are not considered, and the method has been evaluated only through numerical simulations. Future work will investigate more realistic UAV dynamics, alternative observer designs, and real-time experimental validation.

Acknowlegements

This research is funded by the Hanoi University of Science and Technology (HUST) under the project number T2025-PC-050.

References

[1] F. Chen and W. Ren, “On the control of multi-agent systems: A survey”, Foundations and Trends in Systems and Control, vol. 6, no. 4, pp. 339–499, Jul. 2019. DOI: https://doi.org/10.1561/2600000019.

[2] A. Dorri, S. S. Kanhere and R. Jurdak, “Multi-agent systems: A survey”, IEEE Access, vol. 6, pp. 28573–28593, Apr. 2018. DOI: https://doi.org/10.1109/ACCESS.2018.2831228.

[3] Q. Chen, Y. Wang, Y. Jin, T. Wang, X. Nie and T. Yan, “A survey of an intelligent multi-agent formation control”, Applied Sciences, vol. 13, no. 10, Art. no. 5934, May 2023. DOI: https://doi.org/10.3390/app13105934.

[4] Y. Liu, J. Liu, Z. He, Z. Li, Q. Zhang and Z. Ding, “A survey of multi-agent systems on distributed formation control”, Unmanned Systems, vol. 12, no. 5, pp. 913–926, Oct. 2024. DOI: https://doi.org/10.1142/S2301385024500274.

[5] K.-K. Oh, M.-C. Park and H.-S. Ahn, “A survey of multi-agent formation control”, Automatica, vol. 53, pp. 424–440, Mar. 2015. DOI: https://doi.org/10.1016/j.automatica.2014.10.022.

[6] H. T. Do, H. T. Hua, M. T. Nguyen, C. V. Nguyen, H. T. T. Nguyen, H. T. Nguyen and N. T. T. Nguyen, “Formation control algorithms for multiple-UAVs: A comprehensive survey”, EAI Endorsed Transactions on Industrial Networks and Intelligent Systems, vol. 8, no. 27, Art. no. e3, Jun. 2021. DOI: https://doi.org/10.4108/eai.10-6-2021.170230.

[7] C. K. Verginis, A. Nikou and D. V. Dimarogonas, “Position and orientation based formation control of multiple rigid bodies with collision avoidance and connectivity maintenance”, in Proceedings of the 56th IEEE Conference on Decision and Control (CDC), Melbourne, Australia, Dec. 12–15, 2017, pp. 411–416. DOI: https://doi.org/10.1109/CDC.2017.8263699.

[8] X. Hou, S. Guo, Z. Li, H. Shi, N. Yuan and H. Xing, “Design and implementation of a position-based coordinated formation system for underwater multiple small spherical robots”, Oceans, vol. 6, no. 2, Art. no. 21, Apr. 2025. DOI: https://doi.org/10.3390/oceans6020021.

[9] J. A. Fax and R. M. Murray, “Information flow and cooperative control of vehicle formations”, IEEE Transactions on Automatic Control, vol. 49, no. 9, pp. 1465–1476, Sep. 2004. DOI: https://doi.org/10.1109/TAC.2004.834433.

[10] R. Olfati-Saber, J. A. Fax and R. M. Murray, “Consensus and cooperation in networked multi-agent systems”, Proceedings of the IEEE, vol. 95, no. 1, pp. 215–233, Jan. 2007. DOI: https://doi.org/10.1109/JPROC.2006.887293.

[11] R. Olfati-Saber and R. M. Murray, “Consensus problems in networks of agents with switching topology and time-delays”, IEEE Transactions on Automatic Control, vol. 49, no. 9, pp. 1520–1533, Sep. 2004. DOI: https://doi.org/10.1109/TAC.2004.834113.

[12] F. Mehdifar, C. P. Bechlioulis, F. Hashemzadeh and M. Baradarannia, “Prescribed performance distance-based formation control of multi-agent systems”, Automatica, vol. 119, Art. no. 109086, Sep. 2020. DOI: https://doi.org/10.1016/j.automatica.2020.109086.

[13] H. M. Vu, M. H. Trinh, Q. V. Tran and H.-S. Ahn, “Distance-based formation tracking of single- and double-integrator agents”, IEEE Transactions on Automatic Control, vol. 69, no. 2, pp. 1332–1339, Feb. 2024. DOI: https://doi.org/10.1109/TAC.2023.3299817.

[14] M. H. Trinh, S. Zhao, Z. Sun, D. Zelazo, B. D. O. Anderson and H.-S. Ahn, “Bearing-based formation control of a group of agents with leader-first follower structure”, IEEE Transactions on Automatic Control, vol. 64, no. 2, pp. 598–613, Feb. 2019. DOI: https://doi.org/10.1109/TAC.2018.2836022.

[15] S. Zhao and D. Zelazo, “Bearing rigidity and almost global bearing-only formation stabilization”, IEEE Transactions on Automatic Control, vol. 61, no. 5, pp. 1255–1268, May 2016. DOI: https://doi.org/10.1109/TAC.2015.2459191.

[16] L. Chen and M. Cao, “Angle rigidity for multi-agent formations in 3D”, IEEE Transactions on Automatic Control, vol. 68, no. 10, pp. 6130–6145, Oct. 2023. DOI: https://doi.org/10.1109/TAC.2023.3237799.

[17] C. Peng and J. Huang, “Angle-constrained distributed formation control with disturbance rejection”, Automatica, vol. 177, Art. no. 112314, Jul. 2025. DOI: https://doi.org/10.1016/j.automatica.2025.112314.

[18] S. Hyeon, H. Kim and H. Shim, “Data-driven displacement-based formation control with range-only measurements”, IEEE Access, vol. 13, pp. 115167–115177, Jul. 2025. DOI: https://doi.org/10.1109/ACCESS.2025.3584829.

[19] H. G. de Marina, “Maneuvering and robustness issues in undirected displacement-consensus-based formation control”, IEEE Transactions on Automatic Control, vol. 66, no. 7, pp. 3370–3377, Jul. 2021. DOI: https://doi.org/10.1109/TAC.2020.3019780.

[20] E. Sariyildiz, R. Oboe and K. Ohnishi, “Disturbance observer-based robust control and its applications: 35th anniversary overview”, IEEE Transactions on Industrial Electronics, vol. 67, no. 3, pp. 2042–2053, Mar. 2020. DOI: https://doi.org/10.1109/TIE.2019.2903752.

[21] W.-H. Chen, “Disturbance observer based control for nonlinear systems”, IEEE/ASME Transactions on Mechatronics, vol. 9, no. 4, pp. 706–710, Dec. 2004. DOI: https://doi.org/10.1109/TMECH.2004.839034.

[22] L.-X. Xu, Y.-L. Wang, X. Wang and C. Peng, “Distributed active disturbance rejection formation tracking control for quadrotor UAVs”, IEEE Transactions on Cybernetics, vol. 54, no. 8, pp. 4678–4689, Aug. 2024. DOI: https://doi.org/10.1109/TCYB.2023.3324752.

[23] H.-S. Ahn, Formation Control: Approaches for Distributed Agents. Springer, 2020. DOI: https://doi.org/10.1007/978-3-030-15187-4.

[24] T. T. Nguyen, D. V. Vu, T. V. Pham and M. H. Trinh, “Bearing-constrained leader-follower formation of single-integrators with disturbance rejection: Adaptive variable-structure approaches”, IEEE Transactions on Cybernetics, vol. 54, no. 11, pp. 6283–6296, Nov. 2024. DOI: https://doi.org/10.1109/TCYB.2024.3446746.

[25] C. Godsil and G. Royle, Algebraic Graph Theory. Springer-Verlag, 2001. DOI: https://doi.org/10.1007/978-1-4613-0163-9.

[26] S. Aldarmini, A. Vedyakov and M. Kakanov, “Formation control for multi-agent system with disturbances compensation”, IFAC-PapersOnLine, vol. 55, no. 13, pp. 222–227, 2022. DOI: https://doi.org/10.1016/j.ifacol.2022.07.263.